Biosensors and Bioelectronics 140 (2019) 111349

Contents lists available at ScienceDirect

Biosensors and Bioelectronics

journal homepage: www.elsevier.com/locate/bios

Enhanced organic – inorganic heterojunction of polypyrrole@Bi_2WO_6: Fabrication and application for sensitive photoelectrochemical immunoassay of creatine kinase-MB

Li-Bang Zhu[a,b,d,1], Lei Lu[c,d,1], Hai-Yan Wang[d,1], Gao-Chao Fan[b], Yiting Chen[a,*], Jia-Dong Zhang[c,**], Wei-Wei Zhao[d,***]

[a] Ocean College, Minjiang University, Fuzhou 350108, China
[b] Shandong Key Laboratory of Biochemical Analysis, College of Chemistry and Molecular Engineering, Qingdao University of Science and Technology, Qingdao 266042, China
[c] National & Local Joint Engineering Research Center for Deep Utilization Technology of Rock-salt Resource, School of Chemical Engineering, Huaiyin Institute of Technology, Huai'an, Jiangsu 223003, China
[d] State Key Laboratory of Analytical Chemistry for Life Science, School of Chemistry and Chemical Engineering, Nanjing University, Nanjing 210023, China

ARTICLE INFO

Keywords:
Photoelectrochemical
Immunoassay
Organic – inorganic heterojunction
Polypyrrole
Bi_2WO_6
Creatine kinase-MB

ABSTRACT

In this report, enhanced organic – inorganic heterojunction of polypyrrole@Bi_2WO_6 was fabricated and applied for sensitive photoelectrochemical (PEC) immunoassay of creatine kinase-MB (CK-MB). Specifically, hetero-structured polypyrrole@Bi_2WO_6 photoelectrode was prepared and sandwich immunorecognition were integrated for the CK-MB immunoassay. In the detection, with the aid of alkaline phosphate (ALP)-induced biocatalytic precipitation (BCP), the precipitation-dependent suppression of the photocurrent can be recorded due to the impediment of the interfacial mass and electron transfer. On the basis of target-controlled BCP formation, a novel PEC immunoassay could be developed for the sensitive and specific CK-MB detection. This work manifested the great potential of polypyrrole@Bi_2WO_6 heterojunction as a novel platform for PEC bioanalysis development and also a PEC method for CK-MB detection. This work is expected to stimulate more interest in the design and implementation of numerous other organic – inorganic heterojunction for advanced PEC bioanalysis development.

1. Introduction

Photoelectrochemistry (PEC) is a photons-initiated photon-to-electricity conversion process upon a photoactive material with the features of photonic and electrochemical controllability. For biomolecular detection, PEC bioanalysis has low background due to the separation of excitation source from output signal, and been broadly applied in DNA analysis (Da et al., 2017), immunoassays (Zhang et al., 2018) and enzymatic detection (Wang et al., 2017b). Essentially, from the point of photoactive material, a general PEC bioanalysis process comprises photons absorption, charge carrier formation and transfer, as well as surface redox reactions that allow for the photocurrent signaling corresponding to specific bioanalytical purposes. Typically, many nanostructured semiconductor compounds such as CdS quantum dots (QDs) (Wang et al., 2017a) and TiO_2 nanoparticles (NPs) (Li et al., 2017) have been exploited for PEC bioanalysis application. Nonetheless, the limited absorption spectrum and the inclinable recombination of charge carriers go against the photocurrent generation. Nowadays, heterojunction photoelectrodes have attracted more attention since the combination of individual single-component semiconductors could overcome the drawbacks of pure ones (Wang et al., 2018b, 2017b). These systems show tremendous superiority of suppressing charge recombination and also efficient utilization of the light spectrum (Ge et al., 2019; Wang et al., 2019).

Currently, inorganic – inorganic heterojunctions are prevalent in the field of heterojunction photoelectrode development. For example, BiOI/TiO_2 has been reported for anodic PEC inhibition assay of acetylcholine esterase (Zhao et al., 2013). Recently, PbS QDs/NiO

* Corresponding author.
** Corresponding author.
*** Corresponding author.
E-mail addresses: fjcyt@foxmail.com (Y. Chen), jiadongzhang@hyit.edu.cn (J.-D. Zhang), zww@nju.edu.cn (W.-W. Zhao).
[1] These authors contributed to this work equally.

https://doi.org/10.1016/j.bios.2019.111349
Received 29 March 2019; Received in revised form 21 May 2019; Accepted 23 May 2019
Available online 25 May 2019
0956-5663/

photoelectrodes have been developed for cathodic PEC enzymatic glucose sensing (Dai et al., 2017) and probing of tyrosinase activity (Wang et al., 2018a). Compared with the dominance of inorganic heterojunction in this field, the organic – inorganic heterojunctions have been rarely researched. Typically, Antognazza et al. exploited the PdO/APFO-3: PCBM hybrid organic/inorganic nanostructures for highly sensitive PEC detection of dissolved O_2 in aqueous media (Bellani et al., 2015). Wang et al. recently reported the construction of organic polymer dots (Pdots)/inorganic QDs nanodots heterojunctions for PEC bioanalysis of cysteine (Wang et al., 2018c). In light of the great potential in this direction, to develop new inorganic – inorganic heterojunctions would obviously be desirable for high-performance PEC bioanalysis development.

Bismuth tungstate (Bi_2WO_6) represents an attractive visible-light-responsive semiconductor with environmental benignity and high stability. Its properties as a visible-light photocatalyst have recently been intensively investigated (Saison et al., 2013). However, its application in the area of PEC bioanalysis has seldom been implemented. Very recently, Wang et al. reported the development of nitrogen doped graphene QDs decorated Bi_2WO_6 for PEC detection of pentachlorophenol (Hao et al., 2017). Zhang et al. then proposed the use of CdS/Bi_2WO_6 for highly sensitive PEC detection of amyloid beta (Xu et al., 2018). Given the desirable properties exhibited in these Bi_2WO_6-based heterojunctions, of particular interest here is the possibility of developing Bi_2WO_6-based inorganic – inorganic heterojunction for innovative PEC bioassay application. Among various potential organic candidates, the conducting polymer polypyrrole (PPy) has some attractive features in terms of high conductivity, high absorption coefficients in the visible-light region, high mobility of charge carriers, and also excellent stability. It thus is expected to be a good candidate for enhancing the performance of Bi_2WO_6 for advanced PEC bioanalysis. However, such an organic – inorganic heterojunction has yet to be exploited in the field of PEC bioanalysis.

Creatine kinase-MB (CK-MB), one of isoenzymes of the enzyme creatine kinase (CK), is found primarily in heart muscle cells. Increased CK-MB can usually be detected in someone with a heart attack about 3–6 h after the onset of chest pain. Also, CK-MB test may be used as a follow-up test to an elevated creatine kinase in order to determine whether the increase is due to heart damage or skeletal muscle damage. Quantitative detection of CK-MB is thus important and can be generally realized by such as various mass (Winter et al., 1997), ELISA (Kaneko et al., 1996) and high performance liquid chromatography (HPLC) methods (Gupta et al., 1991). While every technique has distinct advantages, each also suffers from its own limitations such as poor sensitivity and high equipment cost. Therefore, accurate, ultrasensitive and low-cost CK-MB detection is highly desirable. To address this, some amperometric and impedimetric protocols have been proposed (Shin et al., 2016). Especially, as advanced electrochemical techniques, electrochemiluminescence (ECL) and PEC bioanalysis are expected for providing new platforms for facile CK-MB detection. Comparing with the exploitation using ECL technique (Hoshino et al., 2016), no work has been done in the counterpart of PEC bioanalysis.

In this work, we reported the fabrication of enhanced organic – inorganic heterojunction of PPy@Bi_2WO_6 and its application for sensitive PEC immunoassay of CK-MB. Specifically, Bi_2WO_6 nanosheets was prepared by hydrothermal synthesis and then applied for fabrication of PPy@Bi_2WO_6 via a photo-oxidative polymerization process (Scheme 1). After the sequential antibody immobilization, antigen capture, binding of the secondary antibody and labeling of alkaline phosphate (ALP), the protein complex was applied for the enzymatic generation of biocatalytic precipitation (BCP), in which ALP would induce the oxidative hydrolyzing transformation of its substrate (5-bromo-4-chloro-3-indoylphosphate) to a precipitation onto the photoelectrode and thus precipitation-dependent suppression of the photocurrent signal. Since the photocurrent reduction was closely related with the target amount, a selective PEC immunoassay could be realized for CK-MB detection. This work features the use of PPy@Bi_2WO_6 heterostructure as a novel PEC bioanalysis platform and also a sensitive method for CK-MB detection, which to our knowledge has not been reported. More generally, the great potential of organic – inorganic heterojunctions was also manifested and is expected to inspire more interests in the design and implementation of numerous other organic – inorganic heterojunctions for advanced PEC bioanalysis development.

2. Experimental section

2.1. Reagents and apparatus

Free creatine-kinase MB Antigen (CK-MB), monoclonal antibody to free CK-MB (CK-MB Ab_1), biotin-labeled monoclonal antibody to free CK-MB (CK-MB Ab_2) were purchased and labeled by Shanghai Linc-Bio Science Co. LTD (Shanghai, China). Streptavidin labeled alkaline phosphatase (ALP-SA) was purchased from Beijing Biosynthesis Biotechnology Co., LTD. Bovine serum albumin (BSA) and 5-bromo-4-chloro-3- indolyl phosphate (BCIP) were obtained from Sigma-Aldrich. Tween 20 was purchased from Amresco. Pyrrole, ascorbic acid (AA), bismuth nitrate pentahydrate ($Bi(NO_3)_3{\cdot}5H_2O$ and sodium tungstate dihydrate ($Na_2WO_4{\cdot}2H_2O$) were purchased from Sinopharm Chemical Reagent Co., Ltd (China). The indium tin oxide (ITO) slices (type N-STN-S1-10) was obtained from China Southern Glass Holding Co., Ltd. (Shenzhen, China).

The ALP-SA were diluted with 0.01 M Tris–HCl (pH 8.0) containing 5 mM $MgCl_2$ and 0.2 mM $ZnCl_2$. And 0.01 M PBS (pH 7.4) containing 0.15 M NaCl was used for the preparation of antigen and antibody as stock solutions. Washing buffer A was prepared by 0.01 M PBS (pH 7.4) containing 0.05% Tween 20. Washing buffer B was prepared by 0.01 M Tris–HCl (pH 7.4) containing 0.05% Tween 20. The blocking buffer was 0.01 M PBS (pH 7.4) containing 3% (w/v) BSA. Ultrapure water (18.2 MΩ cm resistivity at 25 °C, Millier Q) was used in all experiments.

Scanning electron microscopic (SEM) images were recorded by a Hitachi S4800 scanning electron microscope (Hitachi Co., Japan), with a working distance of around 9 mm and a tilting angle of 0°. The UV–vis absorption spectra were obtained on a Shimadzu UV-3600 UV–vis–NIR photospectrometer (Shimadzu Co.). X-ray photoelectron spectroscopy (XPS) was carried out on PHI5000 VersaProbe (ULVAC-PHI Co., Japan). XRD spectra were characterized by powder X-ray diffraction (XRD) [X'TRA, Cu Kα (ARL Co.)].

PEC measurements were performed with a homemade PEC system equipped with a 5 W light-emitting diode lamp emitting at around 415 nm with a power density of 1.6 mW cm^{-2}. The photocurrent was measured on a CHI 660C electrochemical workstation with a three-electrode system: a PPy/Bi_2WO_6/ITO electrode with a geometrical circular area (0.5 cm in diameter) as the working electrode, a Pt wire as the counter electrode, and a saturated Ag/AgCl electrode as the reference electrode. The photocurrent measurements were taken at a constant potential of 0.0 V (vs saturated Ag/AgCl), and 0.1 M phosphate buffer (pH 7.4) was used as the supporting electrolyte for photocurrent measurements.

2.2. Synthesis of Bi_2WO_6

Bi_2WO_6 photocatalyst was prepared by a typical hydrothermal method (Zhang et al., 2014). Firstly, 2 mmol $Bi(NO_3)_3{\cdot}5H_2O$ was dispersed in 20 mL of ultrapure water and 1 mmol $Na_2WO_4{\cdot}2H_2O$ was dissolved in 20 mL deionized water respectively. After that, the above solutions were added together and along with violent magnetic stirring. The mixture was stirring for 30 min until all the reagents dispersed homogeneously. And then, the mixture was sonicated for 20 min at room temperature, followed by transferring into a 50 mL Teflon-lined autoclave. The autoclave was maintained at 160 °C for 20 h, and was allowed to cool naturally. The precipitates were collected and washed with the ultrapure water and anhydrous ethanol for several times.

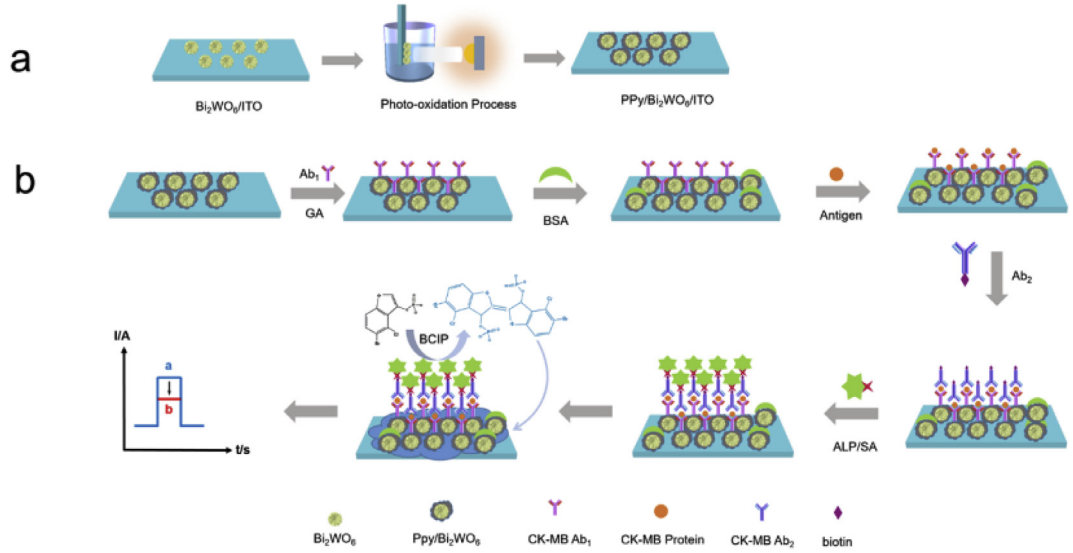

Scheme 1. (a) Preparation of organic – inorganic heterojunction of PPy@Bi_2WO_6 and (b) Application for the PEC immunoassay of CK-MB via an enzymatic BCP process.

Finally, the pure Bi_2WO_6 nanostructures was dried at 60 °C for 12 h.

2.3. Assemble of PPy/Bi_2WO_6 electrodes

Prior to the modification, the ITO conductive glass substrates (0.9 cm × 2.0 cm) were thoroughly boiled in isopropanol/KOH mixed solution (v/v, 1:1) for 30 min, then washed with deionized water. Firstly, the bare ITO was modified with 10 μL Bi_2WO_6 dispersion (5 mg mL^{-1}), drying under environmental atmosphere, then calcination at 400 °C for 1 h in air condition. The PPy@Bi_2WO_6 heterostructure PEC sensor was prepared by 'photo-catalytic oxidative polymerization' process, detail steps as follows: the obtained Bi_2WO_6/ITO electrodes were dipping into the pyrrole aqueous solution (v/v, 1:20000000) with constant stirring. Photo-oxidation was proceeded under a 500 W Xe lamp for 3 h during which pyrrole monomers were oxidized into polypyrrole by the photo induced holes of Bi_2WO_6. The obtained electrode noted as PPy/Bi_2WO_6/ITO.

2.4. Immunoassay development

Ab_1 was immobilized onto the PPy/Bi_2WO_6/ITO was performed via the aldehyde group on glutaraldehyde and the amidogen group on the Ab_1. In detail, the PPy/Bi_2WO_6/ITO was immersed in glutaraldehyde for 1 h, followed by thoroughly rinsing with washing buffer A to wash off the excess glutaraldehyde. Next, the 20 μL 0.2 mg mL^{-1} CK-MB Ab_1 was spread onto the resulting electrode surface and incubated at 4 °C for 12 h. After being washed by buffer A, the electrode was then blocked with 20 μL blocking buffer for 2 h at 4 °C to block non-specific binding sites and washed with the washing buffer A thoroughly. The 20 μL CK-MB with different concentrations was dropped onto the electrodes for an incubation of 1 h at 37 °C followed by washing with buffer A. After rinsed, 20 μL 0.25 mg mL^{-1} CK-MB Ab_2 was spread onto the electrode for another incubation of 60 min at 37 °C.

3. Results and discussions

3.1. Characterization

The SEM images of pure Bi_2WO_6 and PPy@Bi_2WO_6 heterostructure were demonstrated in Fig. 1. As seen in Fig. 1a, large amounts of Bi_2WO_6 nanosheets can be clearly observed. After the PPy modification, as shown in Fig. 1b, the surface of composite became rougher, which could preliminarily prove that the existence of PPy at the surface of Bi_2WO_6 nanosheets. Besides, before and after the PPy modified the Bi_2WO_6/ITO electrode, the color of the electrodes changed from white to black, as shown in insets of Fig. 1a and b.

As shown in Fig. 2a, XRD patterns of the pure Bi_2WO_6 and PPy@Bi_2WO_6 heterostructure were then recorded to investigate the phase structures of the prepared materials. Compared with the pattern of pure Bi_2WO_6, there was no distinct difference on the PPy@Bi_2WO_6 heterostructure, suggesting that the formation of PPy layer on the surface of Bi_2WO_6 did not alter the phase of Bi_2WO_6. To further confirmed the existence of PPy, the full-scan XPS spectra of PPy@Bi_2WO_6 heterojunction was carried out and the result were shown in Fig. 2b. The peaks appeared at ~35.1 eV, 161.1 eV and 529.4 eV corresponded to the W 4f, Bi 4f and O 1s signals, respectively. Especially, the binding energy of N 1s at 443.1 eV can be ascribed to the N element in the PPy, as shown in Fig. 2b inset. The binding energy of 399.6 eV was assigned to neutral pyrrolylium nitrogen (N–H), while the high binding energy peak at 401.5 eV was assigned to the positively charged nitrogen atom ($-N^+$) (Li et al., 2014).

As shown in Fig. 3a, the FT-IR spectra of pure Bi_2WO_6 and PPy@Bi_2WO_6 heterostructure were then performed. As can been seen from the spectrum of pure Bi_2WO_6, main absorption bands at 600–1000 cm^{-1} were observed, which were attributed to Bi–O, W–O stretching and W–O–W bridging stretching modes. The peak at 1381 cm^{-1} was attributed to the bending vibrations of N–O, which may be ascribed to nitrate ions absorbed at the surface of Bi_2WO_6 nanosheets (Duan et al., 2013). Compared with the spectra of pure Bi_2WO_6, there was a remarkable characteristic peak at 1452 cm^{-1} which corresponded to the C=C stretching of the pyrrole rings. And the peak at 1152 and 1048 cm^{-1} were assigned to the characteristic N–C and C–H stretching vibration, respectively. The wide peak observed around 930 cm^{-1} probably was attributed to the = C–H out of plane vibration, indicating the polymerization of pyrrole. As shown in Fig. 3b, UV–vis diffuse reflectance spectra of the samples indicated that the absorption edge of the pure Bi_2WO_6 started from around 450 nm, while the PPy@Bi_2WO_6 composite exhibited an intense absorption in the wide visible light region. These results indicated that the presence of PPy component could significantly enhanced the absorption of the composites in the visible light region.

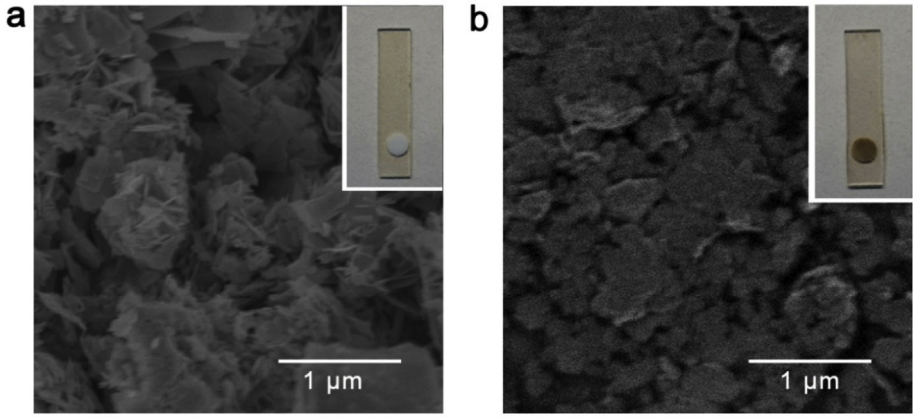

Fig. 1. SEM images of pure Bi_2WO_6 (a) and the PPy@Bi_2WO_6 heterostructure (b) and inset shows the picture of the corresponding modified electrode.

3.2. PEC measurements

To study the light-harvesting properties of the samples, their PEC performances were then probed by chronoamperometric i-t tests upon intermittent light illumination. As shown in Fig. 4a, the presence of PPy could significantly enhance the photocurrent of Bi_2WO_6/ITO electrode. Such an improvement indicated not only the successful modification of PPy but also the strong synergy effect between PPy and Bi_2WO_6. Upon irradiation, as depicted in Fig. 4a inset, the rapid rise of the photocurrent further suggested the fast charge excitation, separation, and transfer in the heterostructure and also the good electrical contact between the Bi_2WO_6 and the ITO glass. Specifically, upon irradiation, both PPy and Bi_2WO_6 could absorb photons that induce charge (e^--h^+) separation with them. The subsequent charge transfer between them can contribute the electron collection by the ITO substrate to generate much enhanced photocurrent. Obviously, such an effect could accelerate the spatial charge separation, prevent the electron−hole recombination, resulting in the increased excitation and conversion efficiency. Fig. 4b shows the effect of PPy polymerization time upon the photocurrent intensities. As shown, 3 h was the optimal time and longer time can cause the photocurrent reduction. Besides, Fig. S1 illustrates the PPy/ITO photocurrent intensities upon illumination (red line) and in the dark (black line). To study the operation stability of the prepared PPy/Bi_2WO_6/ITO electrode, time-based photocurrent response was recorded. As shown in Fig. 4c, the photocurrent intensity did not show any obvious decay under continuous illumination over 400 s. Besides, as shown in Fig. 4c inset, the photocurrent responses were recorded as

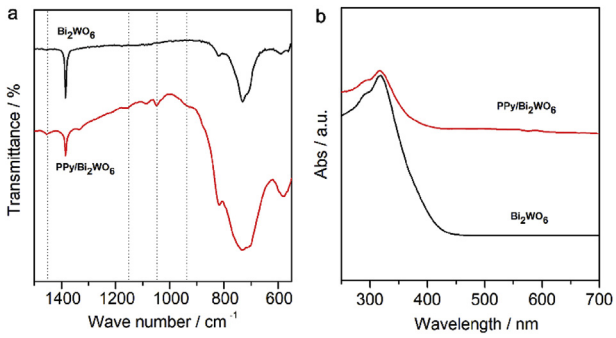

Fig. 3. (a) FT-IR and (b) UV–vis diffuse reflectance spectra of Bi_2WO_6 and PPy@Bi_2WO_6.

the repeated irradiation turned on and off for several cycles, and the electrode displayed reproducible responses without any noticeable decrease during this period, indicating the high photophysical stability of the electrode. Fig. 4d illustrates the anodic photocurrent intensities upon illumination (red line) and in the dark (black line), which increased with the enhanced anodic bias. Given the high bias is harmful to biological samples, 0.0 V vs Ag/AgCl was used as the working voltage in this work.

3.3. Assay feasibility

The stepwise fabrication process of the PEC immunoassay was

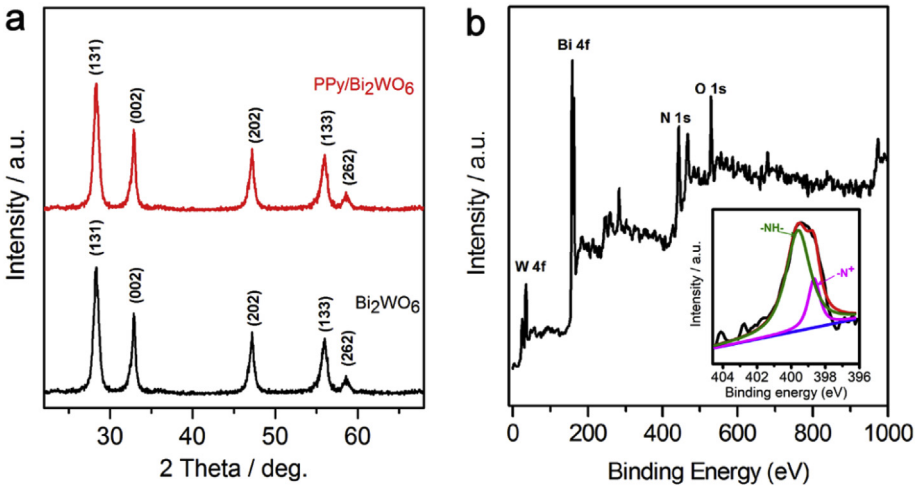

Fig. 2. (a) XRD patterns of Bi_2WO_6 and PPy@Bi_2WO_6 heterostructure. (b) Full-scan XPS spectrum of the PPy@Bi_2WO_6 heterostructure, Inset: the N_{1S} spectrum.

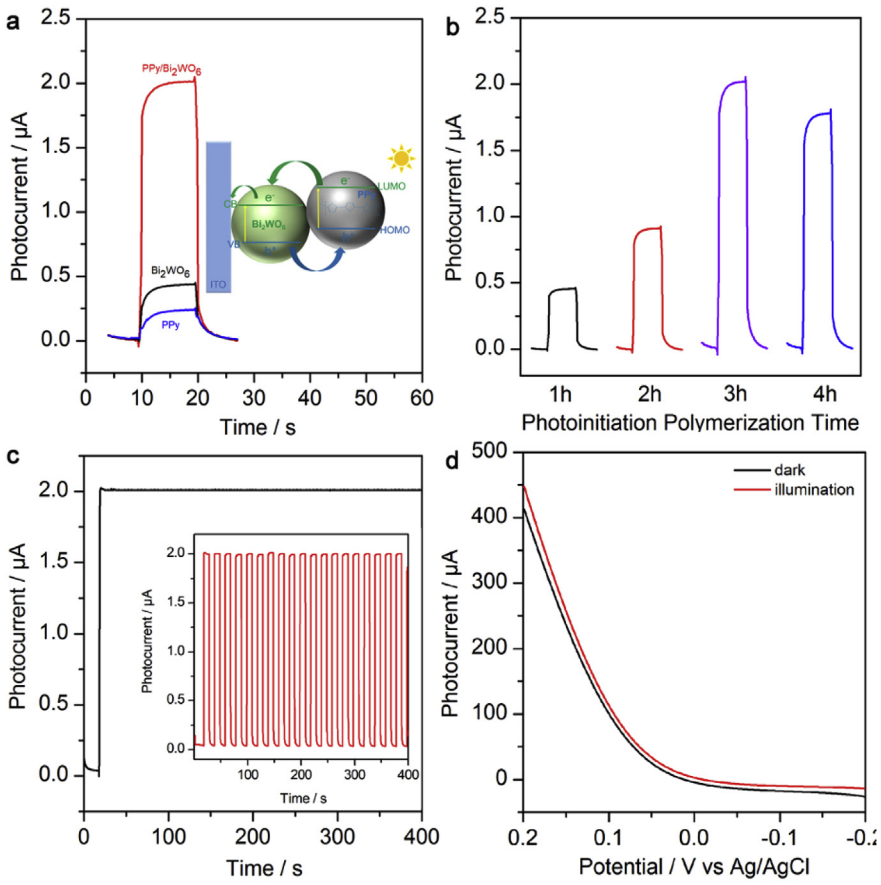

Fig. 4. (a) Photocurrent response of PPy/ITO electrode, Bi_2WO_6/ITO electrode and PPy/Bi_2WO_6/ITO electrode, inset shows the proposed mechanism for the PPy@Bi_2WO_6 enhancement of photocurrent response. (b) Photocurrent of the PPy/Bi_2WO_6 electrode with different time of the photo-catalytic oxidative polymerization. (c) Time-based photocurrent response of the as-fabricated PPy/Bi_2WO_6/ITO electrode. The inset shows the operational stability test by repeated on/off illumination cycles. (d) I–V characteristic curves of the electrode upon illumination (red line) and in the dark (black line) with the range of +0.2 to −0.2 V. (For interpretation of the references to color in this figure legend, the reader is referred to the Web version of this article.)

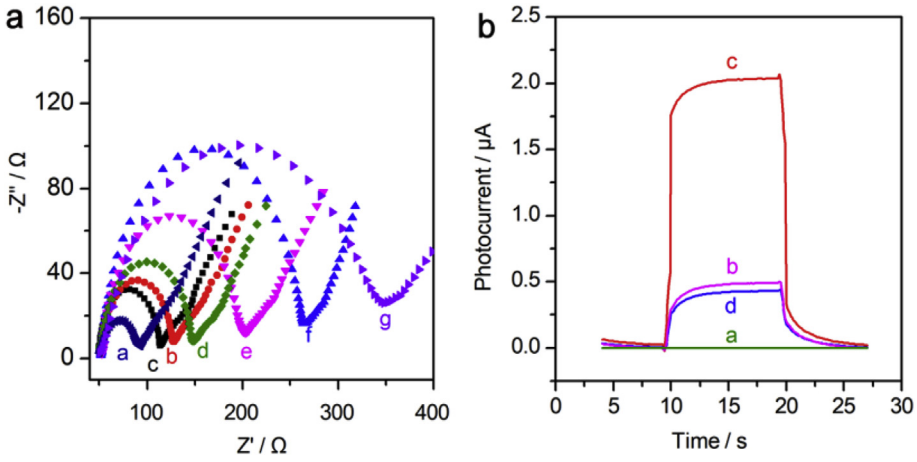

Fig. 5. (a) Nyquist diagrams of (curve a) the bare ITO electrode, (curve b) Bi_2WO_6/ITO electrode, (curve c) PPy/Bi_2WO_6/ITO electrode, (curve d) Ab_1 (0.2 mg mL^{-1})/PPy/Bi_2WO_6/ITO, (curve e) CK-MB/Ab_1/PPy/Bi_2WO_6/ITO, (curve f) Ab_2/CK-MB/Ab_1/PPy/Bi_2WO_6/ITO. (curve g) biotin-ALP/Ab_2/CK-MB/Ab_1/PPy/Bi_2WO_6/ITO. (b) The photocurrents of (curve a) bare ITO, (curve b) Bi_2WO_6/ITO, (curve c) PPy/Bi_2WO_6/ITO, and (curve d) Ab_1/PPy/Bi_2WO_6/ITO electrode after successive incubation with 1000 ng mL^{-1} CK-MB, 0.2 mg mL^{-1} CK-MB Ab_2, 0.2 mg mL^{-1} avidin-ALP and 2 mM BCIP.

characterized by electrochemical impedance spectroscopy (EIS) in 5 mM $Fe(CN)_6^{3-/4-}$ (1:1) solution. As shown in Fig. 5a, the EIS of the bare ITO revealed a relatively small semicircle domain (curve a). With the immobilization of Bi_2WO_6 on ITO electrode, a semi-circle with a R_{et} about 125 Ω (curve b) was observed at high frequency region, which could be ascribed that the diffusion efficiency of the redox probe to electrode was hindered. After the in situ aggregation of PPy (curve c), the R_{et} exhibited slight decrease because of extended p-conjugated electron systems of the PPy. Subsequently, the R_{et} value was further continuously increased when CK-MB Ab_1 (curve d), CK-MB (curve e), CK-MB Ab_2 (curve f) and biotin-ALP (curve g) were successively captured on the electrode surface. It could be attributed to the insulation of immobilized protein that block the transfer of $Fe(CN)_6^{3-/4-}$. The variation of R_{et} along with the development process confirmed the successful fabrication of the biosensor. In order to further study the feasibility, the PEC measurements were also performed. As illustrated in Fig. 5b, no photocurrent response was obtained at the bare ITO electrode (curve a), while an obvious photocurrent was recorded after the Bi_2WO_6 modification (curve b). When the PPy was synthesized on the Bi_2WO_6/ITO surface, a significant photocurrent was produced (curve c), indicating the effective sensitization effect of PPy for Bi_2WO_6. When the PPy/Bi_2WO_6/ITO electrode was successively incubated with 0.2 mg mL^{-1} CK-MB Ab_1, 1 mg mL^{-1} CK-MB, 0.2 mg mL^{-1} CK-MB Ab_2, 0.2 mg mL^{-1} avidin-ALP and 2 mM BCIP, the photocurrent intensity significantly reduced (curve d), confirming the feasibility of the proposed protocol for the PEC detection of the target CK-MB.

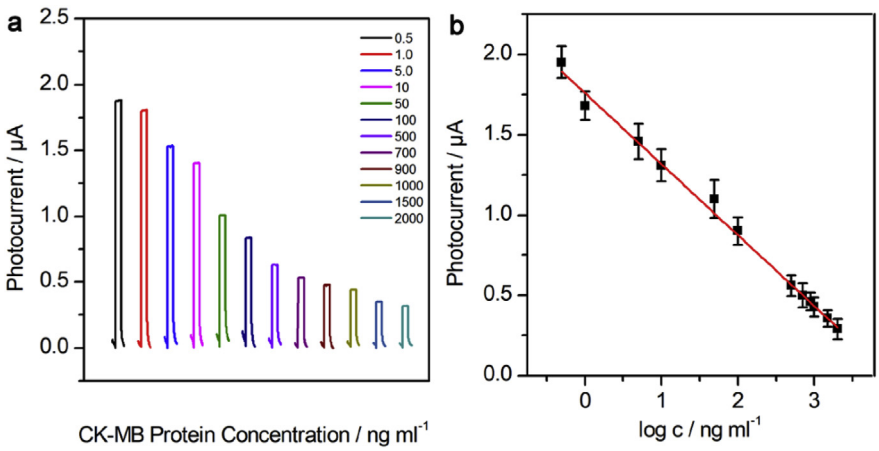

Fig. 6. (a) The photocurrent intensities after BCP, corresponding to increased analyte concentration. The concentrations were 0.5, 1, 5, 10, 50, 100, 500, 700, 900, 1000, 1500, 2000 ng mL^{-1}, respectively. The PEC tests were performed in 0.1 M PBS (pH = 7.4) containing 0.1 M AA with 0 V applied potential and 410 nm excitation. (b) The derived calibration curve.

3.4. Analytical performance

Because the signal variation relates intimately with the CK-MB concentration, the protocol was then optimized, as shown in Fig. S2, and applied for detection of different concentrations of CK-MB. As shown in Fig. 6a, the photocurrent gradually decreased along with increased CK-MB concentrations from 0.5 to 2000 ng mL^{-1}, with the corresponding calibration curve as shown in Fig. 6b. The linear regression equation is I (μA) = −0.4406 log$c$ (ng mL^{-1}) + 1.759 (S/N = 3), with a correlation coefficient 0.995 and the detection limit was estimated to be 0.16 ng mL^{-1}. In addition, we further compared this PEC protocol with other reported works about CK-MB detection. As listed in Table S1, this PEC immunoassay possessed comparable performance among these reported CK-MB assays. The selectivity of the PEC immunoassay was performed by recording the photocurrent responses of the CK-MB, immunoglobulin A (IgA), prostate specific antigen (PSA), carcinoembryonic antigen (CEA), immunoglobulin G (IgG) and fatty acid-binding protein (FABP) in the same conditions. As shown in Fig. S3, it was clearly observed that only CK-MB caused a significant signal change, and the interferents could not cause an obviously signal decrease, indicating the specific binding of the immunocomplex and thus satisfactory selectivity. The stability of the immunoassay system was investigated by storing the sensor at 4 °C for one week and the ΔI remained 97.35% of its original value. The applicability of the system for real sample was also studied as shown in Fig. S4.

4. Conclusion

In this work, we fabricated enhanced organic−inorganic heterojunction of PPy@Bi_2WO_6 and applied it toward sensitive PEC immunoassay of CK-MB. The as-prepared PPy@Bi_2WO_6 was systematically characterized by various techniques, and the PEC measurements demonstrated the good synergy effect between them. In the immunoassay, via the ALP-induced BCP amplification, the system exhibited desirable analytical performance in terms of good sensitivity, selectivity, stability and good applicability for real sample test. These results clearly indicated that the PPy@Bi_2WO_6 heterojunction can be a competitive photoactive platform for the development of advanced PEC immunoassay. This work not only featured the first implementation of PPy@Bi_2WO_6 in PEC immunoassay but also offered a new perspective for the development of numerous other organic−inorganic heterojunction for advanced PEC bioanalytical applications.

Declaration of interests

The authors declare that they have no known competing financial interests or personal relationships that could have appeared to influence the work reported in this paper.

CRediT authorship contribution statement

Li-Bang Zhu: Methodology, Data curation, Formal analysis, Validation, Writing - original draft. **Lei Lu:** Methodology, Data curation, Formal analysis, Validation, Writing - original draft. **Hai-Yan Wang:** Methodology, Data curation, Formal analysis, Validation, Writing - original draft. **Gao-Chao Fan:** Writing - review & editing. **Yiting Chen:** Writing - review & editing, Funding acquisition, Project administration. **Jia-Dong Zhang:** Writing - review & editing, Project administration. **Wei-Wei Zhao:** Conceptualization, Writing - review & editing, Funding acquisition, Project administration.

Acknowledgements

This work was supported by the National Natural Science Foundation of China (Grant Nos. 21605055 and 21675080), the Natural Science Foundation of Jiangsu Province (Grant No. BK20170073) and the Natural Science Foundation of Fujian Province (Grant No. 2019J01757).

Appendix A. Supplementary data

Supplementary data to this article can be found online at https://doi.org/10.1016/j.bios.2019.111349.

References

Bellani, S., Ghadirzadeh, A., Meda, L., Savoini, A., Tacca, A., Marra, G., Meira, R., Morgado, J., Fonzo, F.D., Antognazza, M.R., 2015. Adv. Funct. Mater. 25, 4531–4538.
Da, H., Liu, H., Zheng, Y., Yuan, R., Chai, Y., 2017. Biosens. Bioelectron. 101, 213–218.
Dai, W.X., Zhang, L., Zhao, W.W., Yu, X.D., Xu, J.J., Chen, H.Y., 2017. Anal. Chem. 89, 8070–8078.
Duan, F., Zhang, Q., Shi, D., Chen, M., 2013. Appl. Surf. Sci. 268, 129–135.
Ge, L., Xu, Y., Ding, L., You, F., Liu, Q., Wang, K., 2019. Biosens. Bioelectron. 124–125, 33–39.
Gupta, R.C., Goad, J.T., Kadel, W.L., 1991. Arch. Toxicol. 65, 304–310.
Hao, N., Hua, R., Chen, S., Zhang, Y., Zhou, Z., Qian, J., Liu, Q., Wang, K., 2017. Biosens. Bioelectron. 101, 14–20.
Hoshino, T., Hanai, K., Tanimoto, K., Nakayama, T., 2016. Clin. Lab. 62, 877–885.
Kaneko, N., Matsuda, R., Hosoda, S., Kajita, T., Ohta, Y., 1996. Clin. Chim. Acta 251, 65–80.
Li, X.C., Jiang, G.L., He, G.H., Zheng, W.J., Tan, Y., Xiao, W., 2014. Chem. Eng. J. 236, 480–489.
Li, X., Zhu, L., Zhou, Y., Yin, H., Ai, S., 2017. Anal. Chem. 89, 2369–2376.
Saison, T., Gras, P., Chemin, N., Chanéac, C., Durupthy, O., Brezová, V., Colbeaujustin, C., Jolivet, J.P., 2013. J. Phys. Chem. C 117, 22656–22666.
Shin, S.R., Zhang, Y.S., Kim, D.J., Manbohi, A., Avci, H., Silvestri, A., Aleman, J., Hu, N., Kilic, T., Keung, W., 2016. Anal. Chem. 88, 10019–10027.
Wang, G.L., Yuan, F., Gu, T., Dong, Y., Wang, Q., Zhao, W.W., 2018a. Anal. Chem. 90, 1492–1497.
Wang, H., Yin, H., Huang, H., Li, K., Zhou, Y., Waterhouse, G.I.N., Lin, H., Ai, S., 2018b. Biosens. Bioelectron. 108, 89–96.
Wang, Q., Ruan, Y.F., Zhao, W.W., Lin, P., Xu, J.J., Chen, H.Y., 2018c. Anal. Chem. 90,

3759–3765.
Wang, H., Zhang, Q., Yin, H., Wang, M., Jiang, W., Ai, S., 2017a. Biosens. Bioelectron. 95, 124–130.
Wang, H., Zhu, L., Duan, J., Wang, M., Yin, H., Wang, P., Ai, S., 2017b. Biosens. Bioelectron. 103, 32–38.
Wang, M., Yin, H., Zhou, Y., Sui, C., Wang, Y., Meng, X., Waterhouse, G.I.N., Ai, S., 2019. Biosens. Bioelectron. 128, 137–143.
Winter, R.J., De, Koster, R.W., Straalen, J.P., Van, Gorgels, J.P., Hoek, F.J., Sanders, G.T., 1997. Clin. Chem. 43, 338.
Xu, R., Wei, D., Du, B., Cao, W., Fan, D., Zhang, Y., Ju, H., 2018. Biosens. Bioelectron. 122, 37–42.
Zhang, K., Lv, S., Lin, Z., Li, M., Tang, D., 2018. Biosens. Bioelectron. 101, 159–166.
Zhang, Z., Wang, W., Gao, E., 2014. J. Mater. Sci. 49, 7325–7332.
Zhao, W.W., Shan, S., Ma, Z.Y., Wan, L.N., Xu, J.J., Chen, H.Y., 2013. Anal. Chem. 85, 11686–11690.